ISSN: 2454-9940

INTERNATIONAL JOURNAL OF APPLIED SCIENCE ENGINEERING AND MANAGEMENT

E-Mail :
editor.ijasem@gmail.com
editor@ijasem.org

www.ijasem.org

INTERNATIONAL JOURNAL OF APPLIED SCIENCE ENGINEERING AND MANAGEMENT

ISSN 2454-9940

www.ijasem.org

Vol 19, Issue 2, 2025

Adaptive RCC-Based MPPT for Reliable Solar Energy Harvesting in Dynamic Shaded Scenarios

[1] B.Sahithi,[2] Pandillapalli Ramanjaneyulu Reddy, [3]Alivigonda Siddu, [4]Vasam Venkata Sai Ram,[5] Meenigi Vamsi, [6] Tadimarri Mohammed Shahil,

[1] Assistant Professor, Department of EEE, Ananthalakshmi Institute of Technology and Sciences, Itikalapalli, Near Sk University, Ananthapur.

[2,3,4,5,6]Student, Department of EEE, Ananthalakshmi Institute of Technology and Sciences, Itikalapalli, Near Sk University, Ananthapur.

ABSTRACT

We suggest an iRCC method, which is an improvement on cRCC, such that cRCC can monitor maximum power in both uniform and partial shading conditions (PSC). The proposed iRCC is composed of two components. The first portion is responsible for detecting the global maximum power point (GMPP) under PSC. The second part then operates the photovoltaic (PV) array at GMPP using ripple correlation control. Under conditions of uniform irradiance, the suggested iRCC remains in the second portion; it transitions to the GMPP only in response to dynamic changes in the weather. Both the Matlab simulation and the hardware prototype were used to verify the proposed iRCC. When compared to the standard RCC approach, the performance enhancement is confirmed. The findings demonstrate that, in comparison to the traditional RCC approach, the suggested iRCC algorithm follows the GMPP with more accuracy. Thus, the suggested iRCC approach outperforms the cRCC method by 131% under partial shading condition 1 (PSC-1). The shade caused power peaks at PSC-2, making the suggested iRCC approach's power output almost identical to that of the cRCC method. Based on the shade pattern, it seems that the suggested iRCC approach can achieve better results than the cRCC method. THE SUBSTITUTE WORDS IN THIS INDEX: partial shading condition, ripple correlation control, global maximum power point, and local maximum power point.

INTRODUCTION

There are a number of alternatives to fossil fuels that may be used to generate power, making energy harvesting an essential skill. Renewable wind energy is susceptible to weather fluctuations and may have an effect on local fauna [1]. In addition, it is site-specific, therefore it can't be set up in cities that are too far from the water. Similarly, hydropower is dependable, but it demands massive infrastructure and disturbs ecosystems. Electrical energy harvesting and piezoelectric devices are effective at converting mechanical energy, but they don't provide much power [2, 3, 4]. A similar promising but yet experimental technique is the use of liquid metal in a magnetohydrodynamometer, which is part of the developing field of reverse electrowetting [5, 6, 7]. Several systems exist for capturing solar energy, including photovoltaic (PV), solar thermal, artificial photosynthesis, and molten salt. One renewable energy source that is both environmentally acceptable and continually supplied by nature is solar energy [8, 9, 10, 11, 12]. The inclination towards PV technology is on the rise owing to many benefits [13], which is in line with the ever-increasing need for electrical energy. Solar photovoltaic (PV) panels are arrays of individual PV cells linked in series and parallel to produce usable electricity at a specified power level [14]. The PV system's efficiency, however, is severely affected by weather variations. As irradiance rises, the short circuit current (Isc) in PV panels falls, while open circuit voltage (Voc) falls as temperatures rise, and vice versa [15]. Also, the characteristic curves—namely, the power-voltage (P-V) and current-voltage (I-V) curves—behave non-linearly [16]. Power conditioning circuits are driven by sophisticated algorithms that enable the system to run at maximum power point (MPP). Such programs are known as maximum power point tracking (MPPT) programs [17], [18], [19]. When some panels in a string get less irradiance than the others, a phenomenon known as partial shading occurs, leading to the formation of numerous power peaks. According to references [20], [21], and [22], the highest point is known as the global peak (GP), whereas all the lower peaks are called local peaks (LP). To ensure the system is running as efficiently as possible, monitoring the GP is crucial. It should be noted that traditional maximum power point tracking (MPPT) techniques, such as perturb and observe (P&O) [23], incremental conductance (InC) [25], ripple correlation control (RCC) [26], etc., generally do not perform well in PSC. Actually, these algorithms are unable to follow the GP and instead get stuck at local maxima. In addition to the GMPP, other optimization techniques such as artificial bee colony (ABC) [27], particle swarm optimization (PSO) [28], sliding

mode control (SMC) [29], model predictive control (MPC) [30], and gray wolf optimization (GWO) [31] are used. The processing power and complexity requirements for implementing algorithms based on artificial intelligence (AI) make them challenging to implement. RCC is a time-saving technique for meticulously adhering to the MPP. The authors of the following works have contributed to this article: The inefficiency of cRCC MPPT technology when subjected to partial shade is addressed with a suggested change. • Under all weather circumstances, a two-stage algorithm is shown that can follow the GMPPT. Reducing the size of the duty modulation zone allows for faster MPP tracking, and the suggested iRCC approach can identify GMPP even when the power differential between the two peaks is small. What follows is an outline of the remaining paper. To help new readers understand how a PV module works, Section II presents the single diode model. In Section III, we learn how the load acts when coupled with a PV module using a boost converter. Next, in sections IV and V, respectively, we will go over how the traditional RCC technique and the suggested enhanced RCC method function. There are two ways that the idea validation is carried out. Section VI presents the test scenarios and simulation, whereas Section VII gives the results of the hardware testing. Section VIII provides the conclusion, which concludes the work.

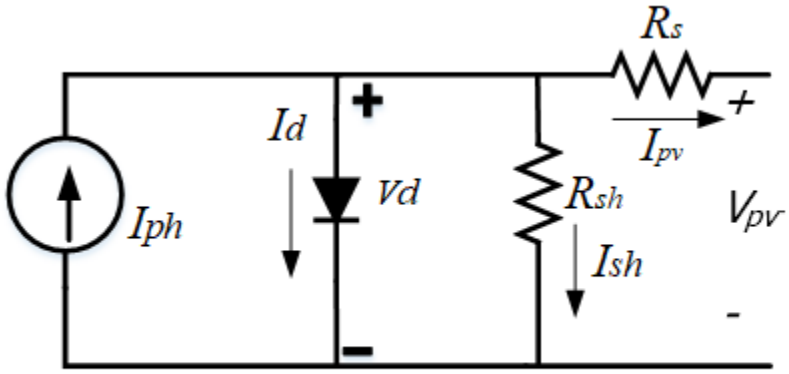

FIGURE 1. Electrical model of a practical PV device.

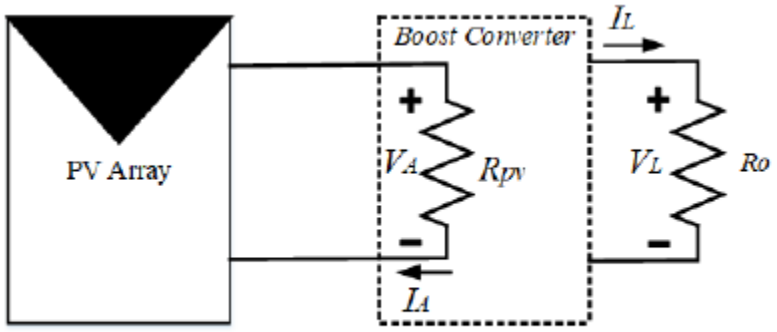

FIGURE 2. Reflection of resistive load on PV through DC-DC converter.

MODELING OF PHOTOVOLTAIC SYSTEM

A PV panel model with a single diode is shown in Figure 1 [32]. It includes a diode for the PN junction, a current source to mimic the photocurrent, and series and shunt resistances to simulate the PV panel's losses. Using the fundamentals of circuit theory, we get equation (1).

$$I_{ph} = I_d + I_{sh} + I_{pv} \qquad (1)$$

in where Iph stands for photocurrent, Id for diodecurrent, Rsh for shunt resistance, and Ipv for output current. Equation (2) is used to determine the current Ish.

$$I_{sh} = \frac{V_d}{R_{sh}} \qquad (2)$$

(3) is where Vd, which stands for the potential difference across the PN junction, is provided.

INTERNATIONAL JOURNAL OF APPLIED SCIENCE ENGINEERING AND MANAGEMENT
ISSN 2454-9940
www.ijasem.org
Vol 19, Issue 2, 2025

$$V_d = V_{pv} + I_{pv}R_s \qquad (3)$$

Using Shockley diode equation, I_d is calculated as eq. (4)

$$I_d = I_0 \exp((V_d/N_sV_t) - 1) \qquad (4)$$

Vt is the thermal voltage, denoted as αKbT/q, where T is the temperature in kelvin, Kb is the Boltzmann constant, q is the charge on the electron, and α is the ideality factor of the diode. Here, I0 is the reverse saturation current of the diode. Below is eq. (5), which is the result of transforming (1) using the formulas in (2) and (4).

$$I = I_{ph} - I_o \exp(q(V_{pv} + I_{pv}R_s)/\alpha K_b T N_s) - 1 \qquad (5)$$

Given the complexity of the problem, solutions to eq.(5) are often derived from numerical analysis or heuristics, as shown in references [33], [34], and [35].

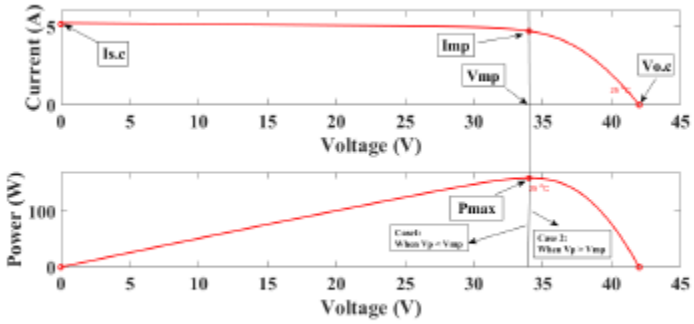

FIGURE 3. Characteristic curves of an arbitrary PV module.

PV INTERFACING WITH BOOST CONVERTER

A switching converter is often used to link a PV device to a load in practical applications. A switching converter adjusts the load's impedance in relation to the PV source's impedance in response to the control input. Rather of being a constant value, the PV array's voltage may range from zero to Voc. The MPPT algorithm changes the value of the duty ratio D to follow the MPP. It is possible to determine the value of D for a dc-dc boost converter by using the formula (6).

$$D_{mp} = 1 - \sqrt{R_{mp}/R_o} \qquad (6)$$

Ro is the load resistance, while Rmp is the product of Vmp and Imp at STC. At MPP, the duty cycle value is Dmp. Additionally, the input-output current has the following relationship, supposing a lossless converter:

$$I_{pv} = I_o/(1 - D) \qquad (7)$$

using the expression for R_{mp} and (7), the relation between the R_{pv} and R_o is expressed as

$$R_{pv} = (1 - D)^2 R_o \qquad (8)$$

The I-V characteristic of the switching converter may be altered by adjusting the duty cycle. Which means the PV system's operating point will vary. Therefore, we can get the load line slope using equation (9)

$$slope = \frac{1}{R_{pv}} \qquad (9)$$

INTERNATIONAL JOURNAL OF APPLIED SCIENCE ENGINEERING AND MANAGEMENT
ISSN 2454-9940
www.ijasem.org
Vol 19, Issue 2, 2025

CONVENTIONAL RIPPLE CORRELATION CONTROL (CRCC) MPPT

RCC makes use of the voltage and current ripple that is already there.

Theoretical optimization as a whole is extensively covered in [36]. In Fig.3, we can see that solar panels operating under uniform irradiance exhibit a power-voltage (P-V) and current-voltage (I-V) characteristic. In instance 1, the change in PV power is positive, while in case 2, it is negative. If the correlation is non-zero, then the power and voltage time derivatives are positive.

Case1:

When $V_{PV} < V_{MP}$

$$(dP/dt)(dV/dt) > 0 \qquad (10)$$

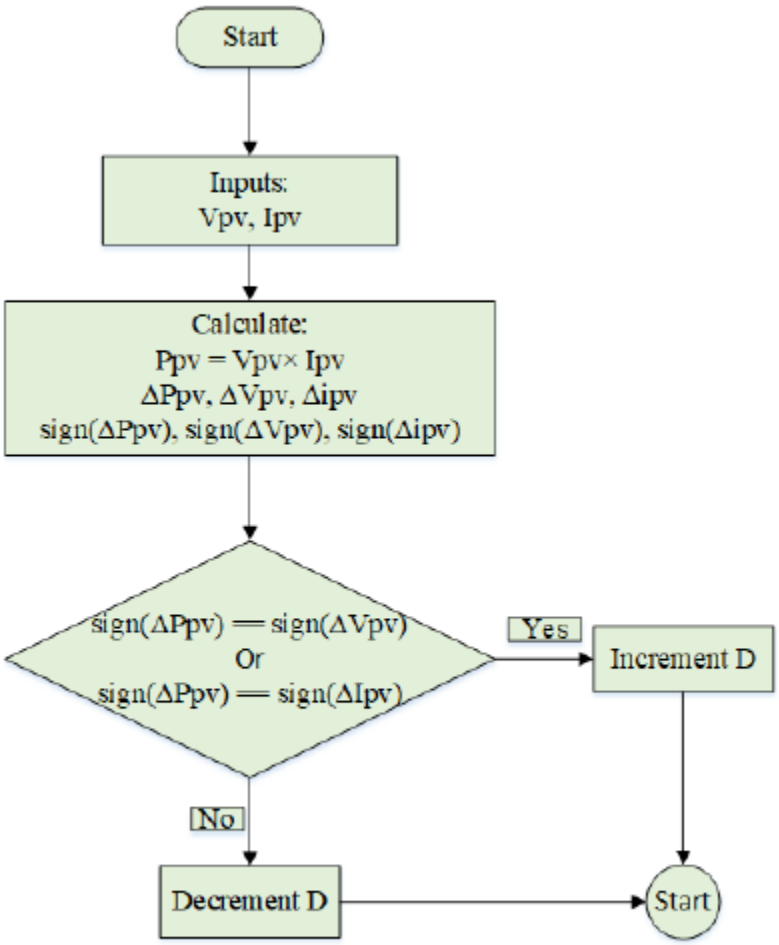

FIGURE 4. Flowchart of conventional RCC MPPT.

Case2:
When $V_{PV} > V_{MP}$

$$(dP/dt)(dV/dt) < 0 \tag{11}$$

$$d = m \int (dP/dt)(dV/dt)dt \tag{12}$$

$$Sign(x) = \begin{cases} -1 & \text{When } x < 0 \\ 0 & \text{When } x = 0 \\ 1 & \text{When } x > 0 \end{cases} \tag{13}$$

$$d = m \int sign(dP/dt)sign(dV/dt)dt \tag{14}$$

If the product of the time-based derivative is more than zero, as it is in instance 1, then the power and voltage ripples are in phase, as shown in equation (10). On the other hand, if the product of the time-based derivative is less than zero, then the ripples are out of phase, as shown in case 2. Equation (12) expresses the relationship between the array voltage and power as a time-based derivative and the duty cycle of the converter. Figure 3 shows the P-V curve, which demonstrates that maximum power point tracking (MPPT) occurs at zero voltage and power derivatives. Modifications to equation (13) are used in more intricate works by integrating the Signum function with respect to the time derivatives of power and voltage [26]. Applying equation (14) to determine the control unit's necessary duty ratio "d" is the foundation of the typical RCC MPPT. To get rid of the differentiation-induced noise, utilize the Sigma function in equation (14) instead. Also, you can figure out the duty ratio by

INTERNATIONAL JOURNAL OF APPLIED SCIENCE ENGINEERING AND MANAGEMENT
ISSN 2454-9940
www.ijasem.org
Vol 19, Issue 2, 2025

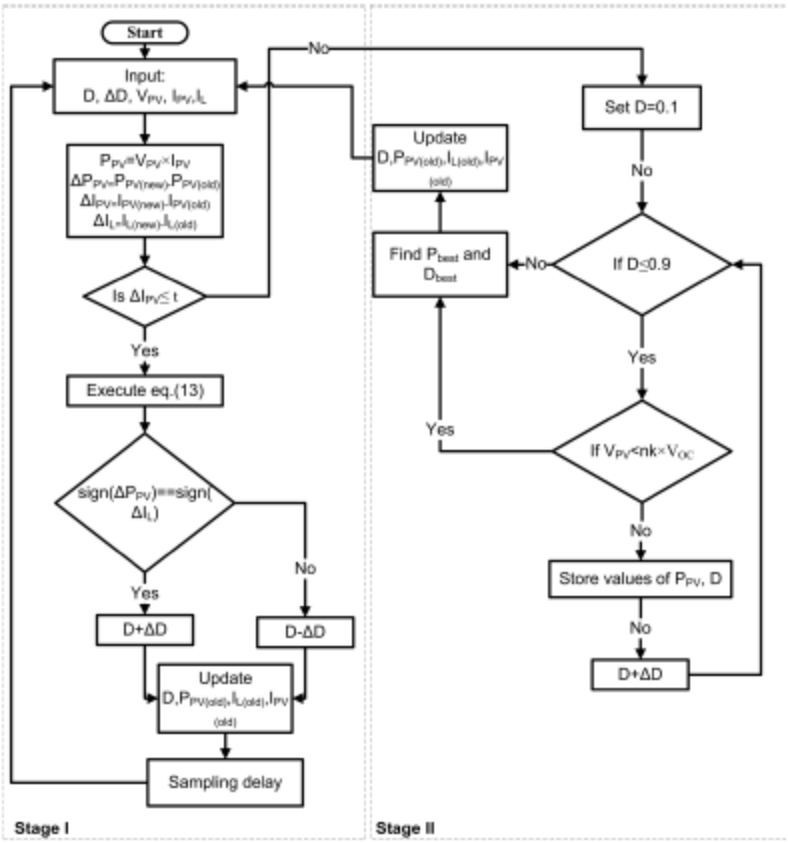

FIGURE 5. Proposed hybrid two stage iRCC algorithm.

voltage-based RCC is thought to be more suited for high-frequency applications, however current-based RCC can also be used [27]. The traditional ripple correlation control technique, as shown in Fig.4, involves sensing the voltage and current, applying the signum function in accordance with eq. (13) and, until the maximum power point PMP is reached, increasing or decreasing the duty cycle correspondingly. When faced with partial shade, the traditional RCC MPPT will not function.

PROPOSED HYBRID TWO STAGE RCC ALGORITHM

Figure 5 shows the flow diagram of the two-stage RCC method that has been suggested. Below, we will go over how these two steps function.

INTERNATIONAL JOURNAL OF APPLIED SCIENCE ENGINEERING AND MANAGEMENT
ISSN 2454-9940
www.ijasem.org
Vol 19, Issue 2, 2025

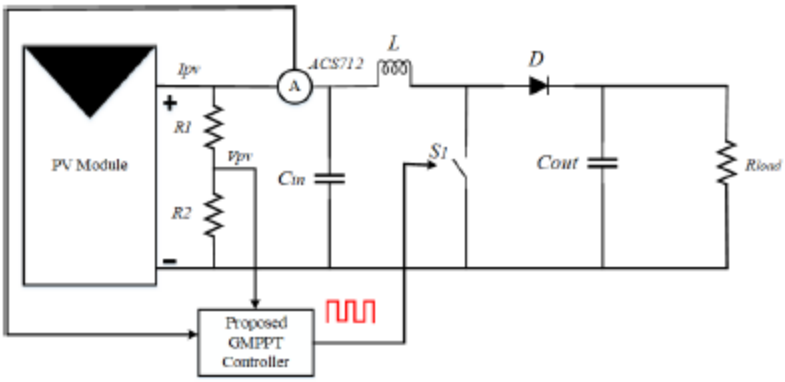

FIGURE 6. Block diagram of proposed algorithm.

CONCEPT VALIDATION

We use lab-built experimental prototypes and computer-aided simulations to verify the suggested change to the RCC MPPT. Figure 6 shows the test bench's overall block design. A 2 x 2 PV array, a dc-dc boost converter, current and voltage sensors, and a controller for creating the MPPT algorithm make up the whole system. The specs for the PV array are shown in Table 1. The PV voltage is sensed by a voltage divider network, and the PV array current is measured using a hall effect sensor. Matlab/Simulink is used to simulate the iRCC method that is suggested. We compare the planned iRCC to the cRCC MPPT for benchmarking purposes. In order to ensure that the proposed RCC MPPT works, the testing settings are not limited to static ambient factors, but also include a variety of partial shade scenarios.

TABLE 1. Data Sheet of PV Module at STC 1000W/m^2, AM 1.5, 25°C.

Parameters	Specification	Values
P_{MP}	Maximum Power Point	40 W
V_{OC}	Open Circuit Voltage	21 V
I_{SC}	Short Circuit Current	2.57 A
V_{MP}	Voltage at MPP	17V
I_{MP}	Current at MPP	2.35A
N_s	No. of series connected cells	60

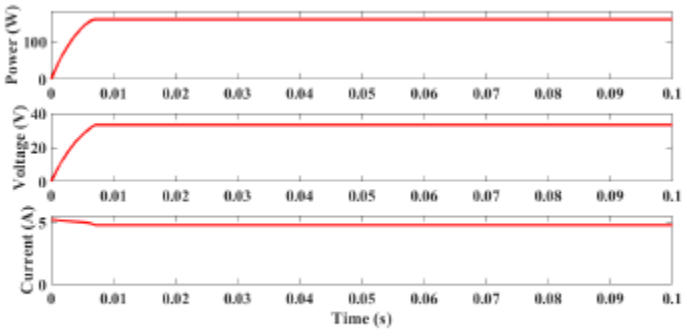

FIGURE 7. Power tracking of two stage algorithm under STC.

INTERNATIONAL JOURNAL OF APPLIED SCIENCE ENGINEERING AND MANAGEMENT
ISSN 2454-9940
www.ijasem.org
Vol 19, Issue 2, 2025

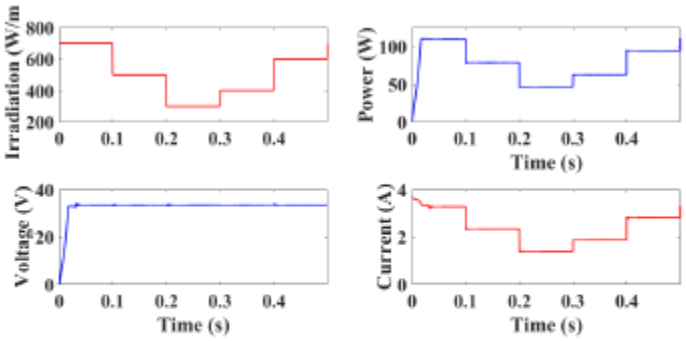

FIGURE 8. Power tracking of the two stage algorithm under variable irradiance.

SIMULATION

Table 2 lists two distinct partial shade situations, in addition to the conventional testing conditions of 1000 W m2 and 25◦C, and variable irradiance. The GMPP occurs on the second peak of the PSC-2 and the first peak of the PSC-1 due to the selection of partial shade circumstances.

TABLE 2. Partial shading scenarios.

Irradiance	G1(W/m^2)	G2(W/m^2)	G3(W/m^2)	G4(W/m^2)
Module	M_{11}	M_{12}	M_{21}	M_{22}
PSC-1	200	200	1000	1000
PSC-2	900	900	600	600

Figure 7 shows that the key waveform obtained under the STC. The proposed system worked well under the STC.

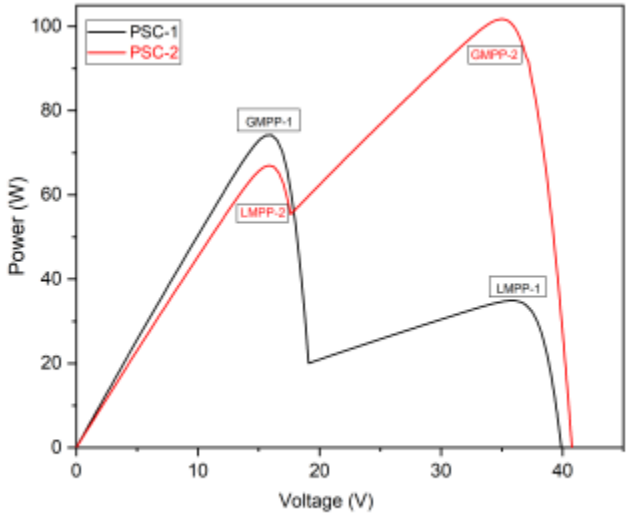

FIGURE 9. Resultant P-V curves under partial shading conditions 1 and 2.

INTERNATIONAL JOURNAL OF APPLIED SCIENCE ENGINEERING AND MANAGEMENT
ISSN 2454-9940
www.ijasem.org
Vol 19, Issue 2, 2025

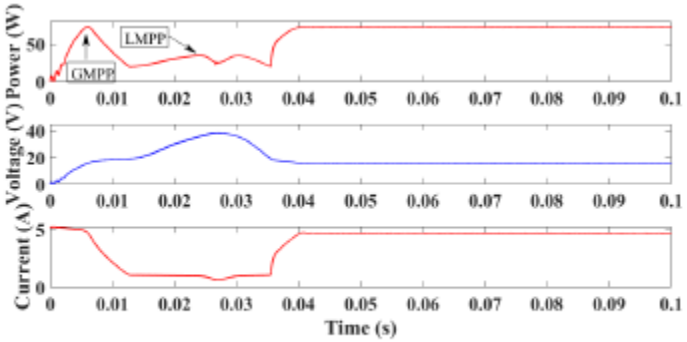

FIGURE 10. Power tracking of the proposed algorithm under PSC-1.

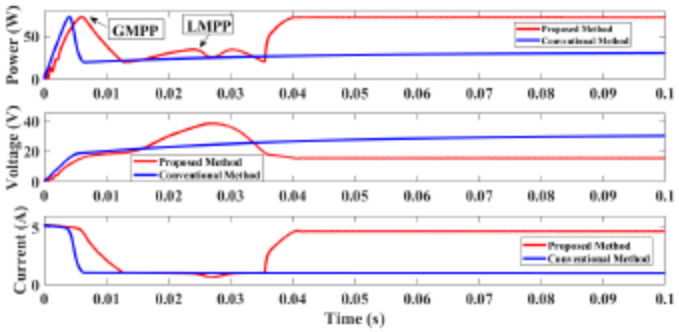

FIGURE 11. Comparison of the proposed and conventional method under PSC-1.

Finding out how well the suggested two-stage method gets to the GMPP is the purpose of this test. Figure 9 shows that the chosen PV panel scheme experiences two power peaks in the P-V curves when exposed to the partial shadowing circumstances from table 2. Figure 10 shows that the suggested two-step approach can run the system at GMPP because it include a partial shading detection stage. As seen in the relevant power curve of the system in Fig.12, the algorithm identifies the peaks according to the proposed technique before operating the system at the GMPP when PSC-2 is applied to the system. Table 3 summarizes the performance gain of the suggested hybrid two stage approach.

TABLE 3. Comparison of the proposed and conventional method for PSC-1 and PSC-2.

Method	P_{max}(W)	Photovoltaic Power (W)	Tracking time (ms)	Tracking efficiency (in percent)
Proposed Method	72.91 for PSC-1	72.57	40	99.53
Conventional Method	72.91 for PSC-1	31.38	200	43.03
Proposed Method	101 for PSC-2	100.6	27.2	99.60
Conventional Method	101 for PSC-2	100.3	30.76	99.30

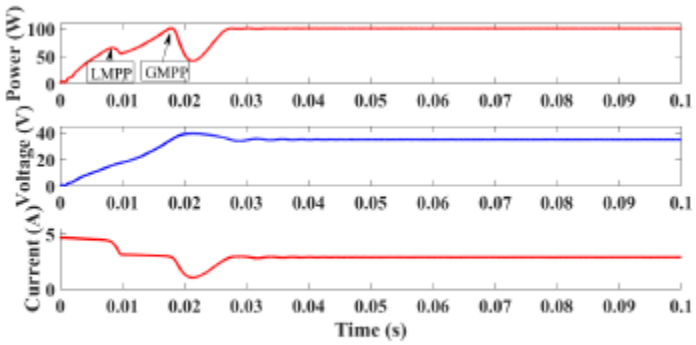

FIGURE 12. Power tracking of the proposed algorithm under PSC-2.

INTERNATIONAL JOURNAL OF APPLIED SCIENCE ENGINEERING AND MANAGEMENT
ISSN 2454-9940
www.ijasem.org
Vol 19, Issue 2, 2025

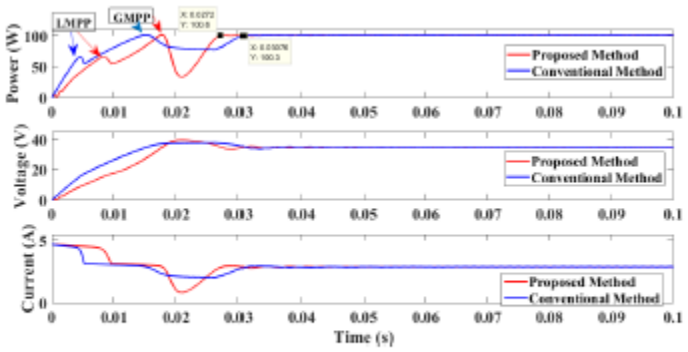

FIGURE 13. Comparison of the proposed and conventional method under PSC-2.

While traditional methods similarly employ two sensors—voltage and current—to give the duty cycle, the suggested approach uses three. The standard and suggested methods both make use of a single diode and mosfet. When compared to the suggested technique, the traditional one has a relatively low level of complexity. No matter how subtle the tint, the suggested approach responds correctly. When faced with partial shading, the usual method's response is inaccurate. Figure 11 displays the time of irradiation such that the first peak is GMPP. Regardless of whether it is not GMPP, the traditional approach stays at the 2nd peak, as seen in Fig. 11. Here, the suggested approach clings to the GMPP peak, while the traditional method continues to draw power from the second peak at a lower level. When a partial darkening has taken place, as seen in Fig.13, the second peak will be GMPP. In this instance, the GMPP serves as a peak that is followed by both the traditional and suggested approaches. As seen in Figure 13, the usual technique requires a significant amount of time for tracking. The suggested approach has a short tracking time. While the standard approach has a short settling time, the suggested method has a high one.

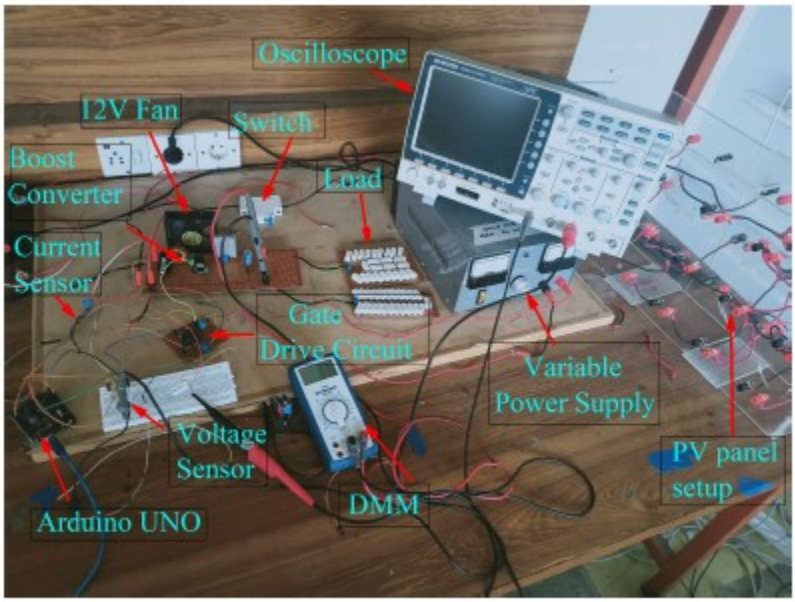

FIGURE 14. Experimental setup.

Table 3 compares the suggested technique to the standard method for a number of factors. While 72.91 W is the nominal power in the partly shadowed condition PSC-1, the power track according to the suggested technique is 72.57 W. In contrast, the power track using the traditional approach is 31.38 W. When comparing the two methods, the suggested one has a settling time of 40 ms, whilst the traditional one takes 200 ms. Next, we have PSC-2 with a nominal power of 101 W and a power track of 100.6 W using the suggested approach, with a settling time of 27.2 ms. With a settling time of 30.7 ms, the power trace in the PSC-2, according to the standard technique, is 100.3 W. Finally, after looking at the outcomes of both methods under various PSCs. Whereas the traditional approach fails under a variety of PSC conditions, the suggested technique is applicable to tracking the

INTERNATIONAL JOURNAL OF APPLIED SCIENCE ENGINEERING AND MANAGEMENT
ISSN 2454-9940
www.ijasem.org
Vol 19, Issue 2, 2025

rated power under all PSC types. The suggested strategy outperforms the standard way in terms of tracking speed regardless of the presence or absence of PSCs. In comparison to the standard technique, the suggested approach is more efficient under all PSCs.

EXPERIMENTAL VALIDATION

Figure 14 shows the experimental verification of the proposed two-stage hybrid method utilizing a hardware prototype. Table 4 lists the values of the important parts of this configuration. A voltage divider network (ACS712 20) is used to detect the voltage, however. To measure the current, a current sensor is used. The suggested method is executed by a microcontroller that interacts with the output of these sensors. The gate driver circuit receives the required switching pulse from the suggested technique in order to activate the GMPPT. The experimental results show that the standard method | FIGURE 18 | performs adequately. Situation with partial shade 1. FILE 19: Condition of partial shading II.

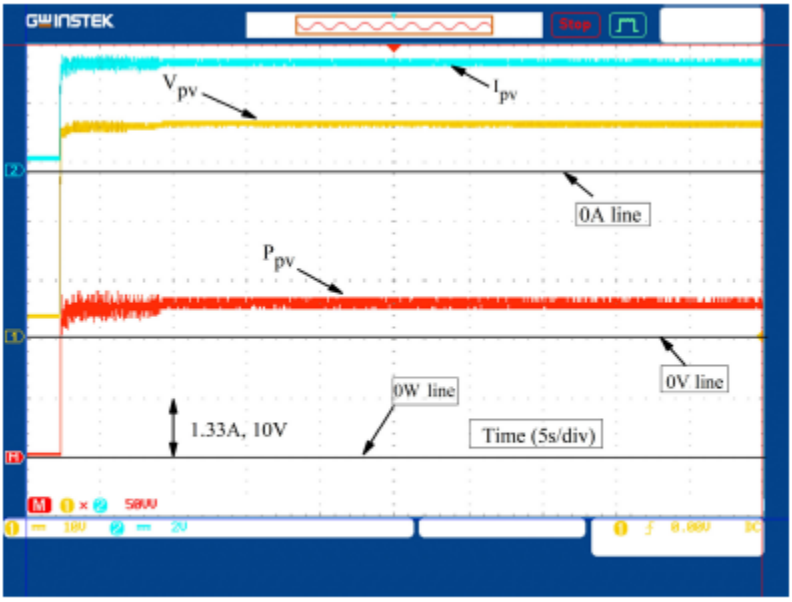

FIGURE 15. Experimental results for uniform irradiance condition.

INTERNATIONAL JOURNAL OF APPLIED SCIENCE ENGINEERING AND MANAGEMENT
ISSN 2454-9940
www.ijasem.org
Vol 19, Issue 2, 2025

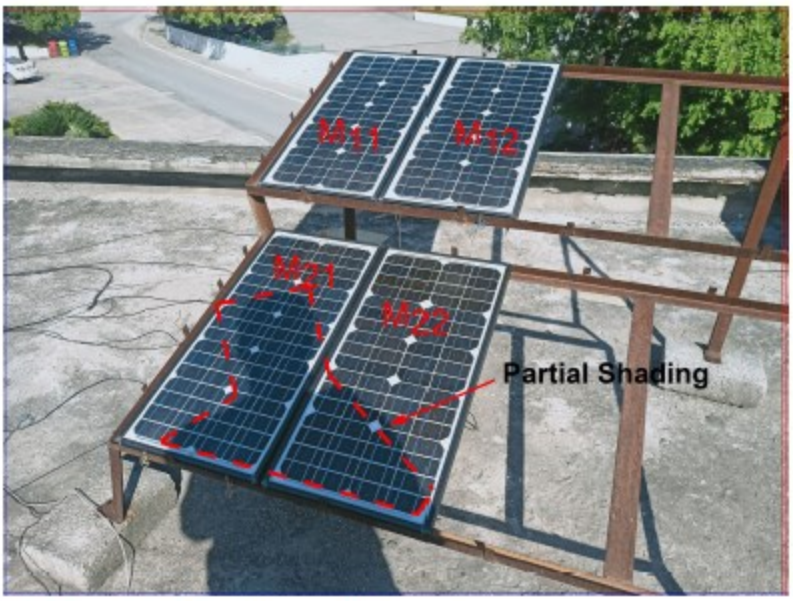

FIGURE 16. Partial shading condition 1 (PSC-1).

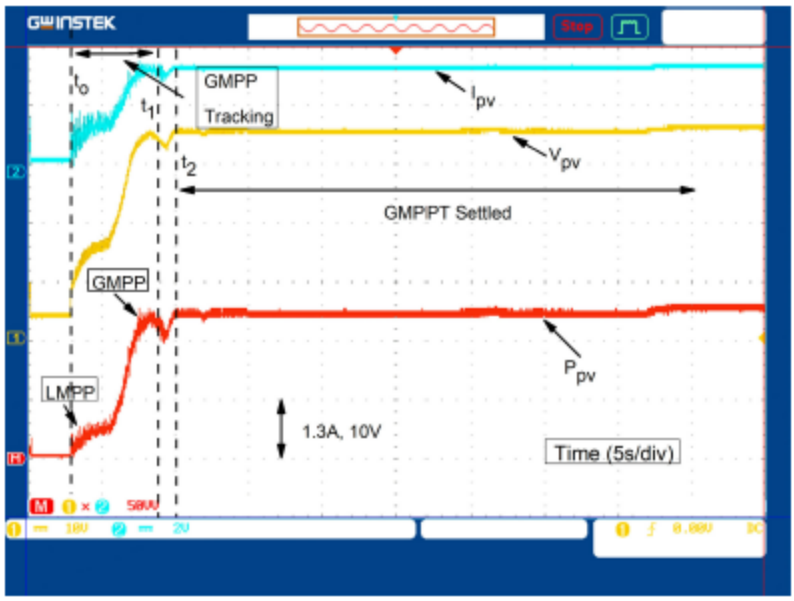

FIGURE 17. Performance of proposed algorithm | Partial shading condition 1.

As part of the verification procedure, the proposed hybrid algorithm is benchmarked against the standard RCC MPPT approach.

INTERNATIONAL JOURNAL OF APPLIED SCIENCE ENGINEERING AND MANAGEMENT
ISSN 2454-9940
www.ijasem.org
Vol 19, Issue 2, 2025

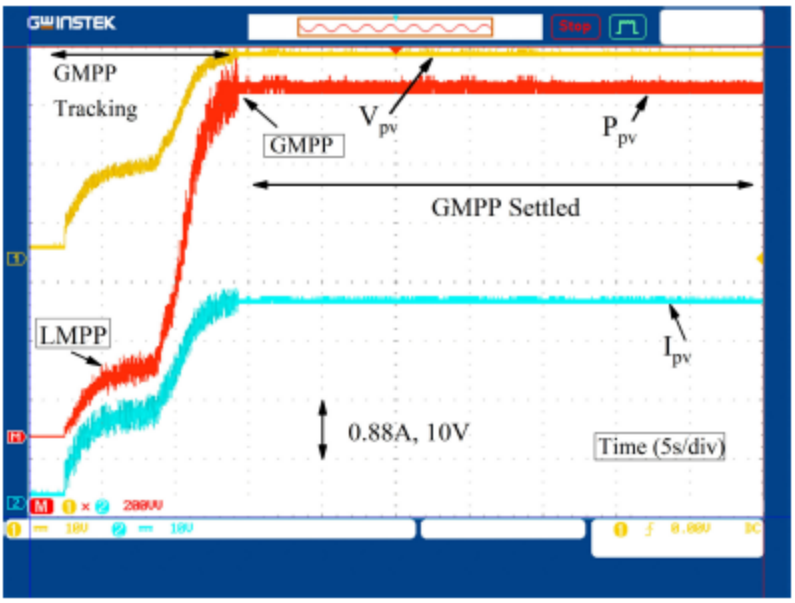

FIGURE 18. Performance of conventional algorithm | Partial shading condition 1.

FIGURE 19. Partial shading condition II.

Figure 15 displays the hardware results of the suggested method when evaluated under uniform irradiance conditions, after the simulation test. Then, the partial shading tests are run. In Figure 16, we can see the PSC-1

INTERNATIONAL JOURNAL OF APPLIED SCIENCE ENGINEERING AND MANAGEMENT
ISSN 2454-9940
www.ijasem.org
Vol 19, Issue 2, 2025

implementation, which involves casting a human shadow on panels M21 and M22 while leaving panels M11 and M12 shadowless. As can be seen in Figure 17, this situation of partial shading results in a P-V curve with the GMPP located on the second peak.

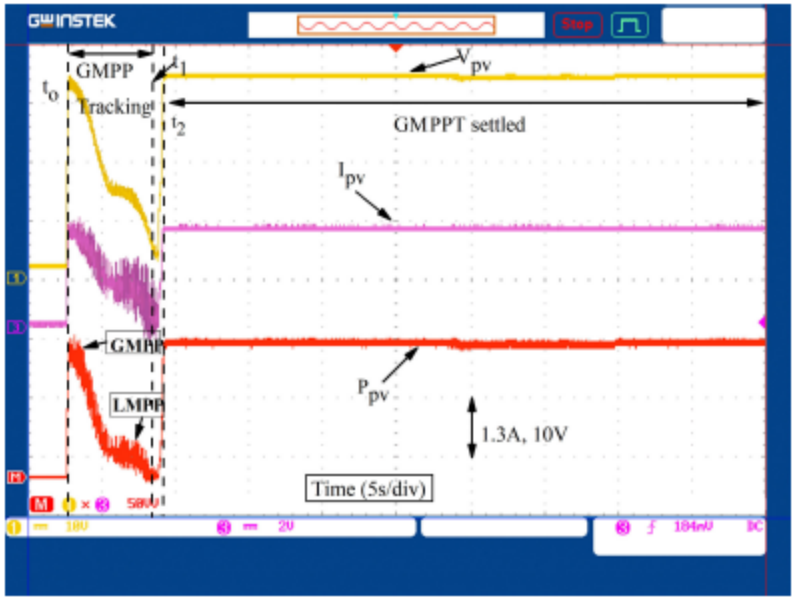

FIGURE 20. Performance of proposed algorithm | Partial shading condition 2. (PSC-2).

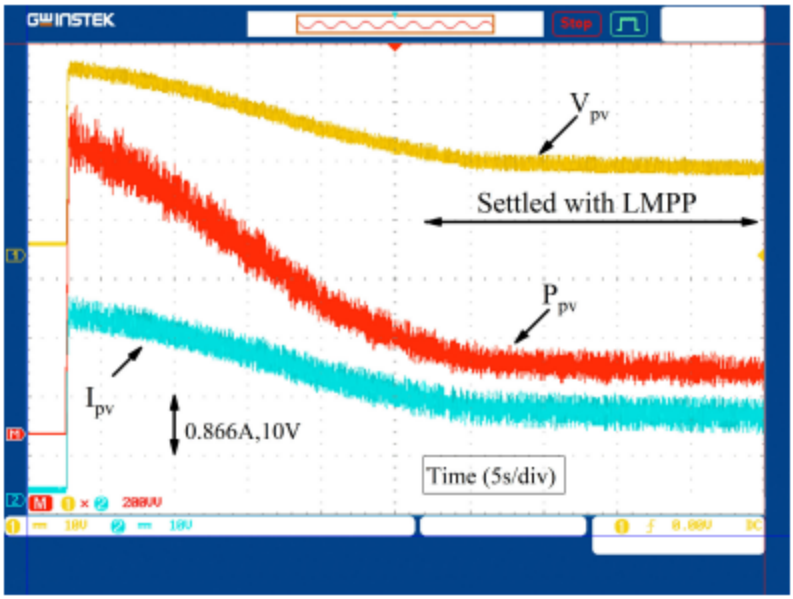

FIGURE 21. Performance of conventional algorithm | Partial shading condition 2.

TABLE 4. Detail of prototype components.

Components	Variable	Value
2X2 array		Table ??
Inductor	L	160 μH
Input Capacitor	C_{in}	1000 μF
Output Capacitor	C_{out}	47 μF
Load Resistance	R_L	63 Ω

Figure 18 elaborates on the performance of the standard RCC method for the identical partial shading case. The second situation shown in Figure 19 is the partial darkening that causes the first peak to generate GMPP. Panels M21 and M22 are shadow-free, whereas panels M11 and M12 are engulfed in the artificial shadow. Experimental results for the suggested hybrid two-stage approach are shown in Figure 20. The first step, based on duty modulation, identifies the global maxima from t0 to t1. The second stage, based on RCC, to stay with the GMPP, is initiated from t1 to t2. Conversely, Fig.21 shows the results of traditional RCC MPPT under the same partial shadowing condition. It is evident that the traditional RCC MPPT algorithm continues to function at the second peak, LMPP, even when the meteorological conditions alter. The efficiency of the suggested approach, as compared to the usual RCC method, is shown by this experimental verification.

CONCLUSION

This paper proposes an iRCC method for reaching the highest power point on a global scale. Evidence from a variety of real-world tests shows that the suggested technique can function even when partially shaded. Analysis of the results leads us to the following conclusion: The suggested iRCC approach efficiently tracks the GMPP. Whereas, depending on the shading pattern, the typical cRCC could or might not follow the GMPP.

REFERENCES

[1] M. Waseem, Y. Feng, Y. Qiu, C. Sun, and H. A. Sher, ‘‘Improved vector current control for grid side converter in PMSG wind turbine with fault tolerance capability,’’ in *Proc. 8th Renew. Power Gener. Conf. (RPG)*. IET, Oct. 2019, pp. 1–8.
[2] P. Muralt, M. Marzencki, B. Belgacem, F. Calame, and S. Basrour, ‘‘Vibration energy harvesting with PZT micro device,’’ *Proc. Chem.*, vol. 1, no. 1, pp. 1191–1194, Sep. 2009.
[3] A. Crovetto, F. Wang, and O. Hansen, ‘‘Modeling and optimization of an electrostatic energy harvesting device,’’ *J. Microelectromech. Syst.*, vol. 23, no. 5, pp. 1141–1155, Oct. 2014.
[4] A. Toprak and O. Tigli, ‘‘Piezoelectric energy harvesting: State-of-the-art and challenges,’’ *Appl. Phys. Rev.*, vol. 1, no. 3, Sep. 2014, Art. no. 031104.
[5] S. R. Gupta, J. A. Taylor, and T. Krupenkin, ‘‘Three-phase alternating current liquid metal vortex magnetohydrodynamic generator,’’ *IScience*, vol. 24, no. 6, Jun. 2021, Art. no. 102644.
[6] S. R. Gupta, I. Matos, T.-H. Hsu, J. A. Taylor, and T. Krupenkin,‘‘Mechanical energy harvesting using combined reverse electrowetting and electromagnetic method,’’ *Device*, vol. 1, no. 1, Jul. 2023, Art. no. 100005.
[7] S. R. Gupta, J. Ashley Taylor, and T. Krupenkin, ‘‘Theoretical investigation of a novel three-phase alternating current liquid metal vortex magnetohydrodynamic generator,’’ *Sustain. Energy Technol. Assessments*, vol. 53, Oct. 2022, Art. no. 102436.
[8] M. A. Bhuiyan, Q. Zhang, V. Khare, A. Mikhaylov, G. Pinter, and X. Huang, ‘‘Renewable energy consumption and economic growth nexus—A systematic literature review,’’ *Frontiers Environ. Sci.*, vol. 10, p. 412, Apr. 2022.
[9] M. N. Gull, T. A. Cheema, A. Imran, N. U. Zaman, H. A. Sher, and C. W. Park, ‘‘Multiphysics performance evaluation of thermoelectric generator arrays,’’ *Appl. Thermal Eng.*, vol. 249, Jul. 2024, Art. no. 123348.
[10] H. Dinçer, S. Yuksel, A. Mikhaylov, S. E. Barykin, T. Aksoy, and Ü. Hacioglu, ‘‘Analysis of environmental priorities for green project investments using an integrated Q-Rung orthopair fuzzy modeling,’’ *IEEE Access*, vol. 10, pp. 50996–51007, 2022.
[11] M. A. Bhuiyan, H. Dinçer, S. Yuksel, A. Mikhaylov, M. S. S. Danish, G. Pinter, D. D. Uyeh, and D. Stepanova, ‘‘Economic indicators and bioenergy supply in developed economies: QROF-DEMATEL and random forest models,’’ *Energy Rep.*, vol. 8, pp. 561–570, Nov. 2022.

[12] J. Li, S. Yuksel, H. Dinçer, A. Mikhaylov, and S. E. Barykin, ‘‘Bipolar q-ROF hybrid decision making model with golden cut for analyzing the levelized cost of renewable energy alternatives,’’ *IEEE Access*, vol. 10, pp. 42507–42517, 2022.
[13] J. Liu, Z. Ye, L. Zhang, X. Fang, and Z. Zhang, ‘‘A combined numerical and experimental study on graphene/ionic liquid nanofluid based direct absorption solar collector,’’ *Sol. Energy Mater. Sol. Cells*, vol. 136, pp. 177–186, May 2015.
[14] M. Dali, J. Belhadj, X. Roboam, and J. M. Blaquiere, ‘‘Control and energy management of a wind-photovoltaic hybrid system,’’ in *Proc. Eur. Conf. Power Electron. Appl.*, 2007, pp. 1–10.
[15] C. F. Abe, J. B. Dias, G. Notton, and P. Poggi, ‘‘Computing solar irradiance and average temperature of photovoltaic modules from the maximum power point coordinates,’’ *IEEE J. Photovolt.*, vol. 10, no. 2, pp. 655–663, Mar. 2020.
[16] M. A. G. de Brito, L. Galotto, L. P. Sampaio, G. D. A. E. Melo, andC. A. Canesin, ‘‘Evaluation of the main MPPT techniques for photovoltaic applications,’’ *IEEE Trans. Ind. Electron.*, vol. 60, no. 3, pp. 1156–1167, Mar. 2013.
[17] J. C. Teo, R. H. G. Tan, V. H. Mok, V. K. Ramachandaramurthy, and C. Tan, ‘‘Impact of partial shading on the P-V characteristics and the maximum power of a photovoltaic string,’’ *Energies*, vol. 11, no. 7, p. 1860, Jul. 2018.
[18] A. M. Noman, H. Khan, H. A. Sher, S. Z. Almutairi, M. H. Alqahtani, and A. S. Aljumah, ‘‘Scaled conjugate gradient artificial neural networkbased ripple current correlation MPPT algorithms for PV system,’’ *Int. J. Photoenergy*, vol. 2023, pp. 1–8, Jun. 2023.
[19] A. F. Murtaza, H. A. Sher, F. Spertino, A. Ciocia, A. M. Noman, A. A. Al-Shamma’a, and A. Alkuhayli, ‘‘A novel MPPT technique based on mutual coordination between two PV modules/arrays,’’ *Energies*, vol. 14, no. 21, p. 6996, Oct. 2021.
[20] R. Ahmad, A. F. Murtaza, H. A. Sher, U. T. Shami, and S. Olalekan, ‘‘An analytical approach to study partial shading effects on PV array supported by literature,’’ *Renew. Sustain. Energy Rev.*, vol. 74, pp. 721–732, Jul. 2017.